Cross sections for ionization of inner-shell electrons by electrons*

C. J. Powell

National Bureau of Standards, Washington, D.C. 20234

A survey is given of the available cross-section data for ionization of inner-shell electrons by incident electrons in the range of interest for electron-probe microanalysis and for Auger-electron spectroscopy of solid surfaces. Owing to the paucity of data, the bulk of the discussion is limited to K-shell and L-shell ionization of light atoms. Calculated, semiempirical, and experimental cross-section data have been intercompared graphically and through fits to the linearized Bethe equation for inner-shell ionization (the Fano plot). Almost all of the data could be satisfactorily fitted over the range $4 \lesssim U_{nl} \lesssim 30$, where $U_{nl} = E_0/E_{nl}$, E_0 is the incident electron energy, and E_{nl} the binding energy of electrons in the nl shell. From these fits, values could be obtained of the "effective" Bethe parameters b_{nl} and c_{nl}. Values of the parameter b_{nl} have also been derived from photoabsorption data and were found to be generally consistent with the ionization data if account was taken of the distribution of differential oscillator strength with respect to excitation energy and the consequent expected variation of b_{nl} with incident electron energy. The derived "effective" Bethe parameters should not therefore be used outside the range of each fit.

CONTENTS

I. INTRODUCTION

There is a large literature dealing with electron-impact ionization cross sections; see, for example, the reviews by Kieffer and Dunn (1966), Mohr (1968), Rudge (1968), Kieffer (1969), Massey and Burhop (1969), Ehrhardt *et al.* (1972), van der Wiel (1973), Cooper (1973), Bell and Kingston (1974), and Madison and Merzbacher (1975). Much of this literature is concerned with the cross sections for the removal of a *valence* electron from a free atom or molecule to produce an ion. Cross sections of this type are used extensively in plasma physics, mass spectroscopy, atmospheric physics, and astrophysics.

This review is concerned with cross sections for the removal of *inner-shell* or core electrons by electron impact. Cross sections of this type are used in two common methods of elemental analysis, electron-probe microanalysis (EPMA) and Auger-electron spectroscopy (AES); in addition, these cross sections will be needed for elemental analysis by measurement of the inner-shell energy-loss spectra of electrons transmitted through samples in the electron microscope (Isaacson and Johnson, 1975). In EPMA, a solid sample is bombarded by an electron beam of energy usually between 5 and 30 keV. This bombardment produces inner-shell vacancies that can decay either by characteristic x-ray emission or by Auger-electron emission (Bambynek *et al.*, 1972). Measurements of the x-ray intensity in EPMA are used to derive elemental concentrations, as described, for example, by Birks (1971), Reuter (1971), Andersen (1972), Hutchins (1974), Lifshin (1974), Yakowitz (1974), and Reed (1975). In AES, the solid sample is usually bombarded by electrons of energy between 2 and 10 keV and the characteristic Auger electrons are used for elemental identification. At the present time, procedures analogous to those in EPMA to convert a measured Auger-electron intensity to an elemental concentration have not been as extensively developed (Seah, 1973; Palmberg, 1973; Riviere, 1973; Chang, 1974; Staib and Kirschner, 1974; Chang, 1975; Morabito, 1975; Vrakking and Meyer, 1975). This situation is due in part to the novelty of AES compared to EPMA and in part to the lack of knowledge of the relevant physical parameters needed for quantitative AES.[1]

We are interested here in cross sections for the production of inner-shell *vacancies*. The term ionization cross section (denoted σ_i) will be used to refer exclusively to the cross section for the production of a vacancy in a particular (the ith) inner shell. Values of σ_i can thus be used to predict the yield of x rays in EPMA or of Auger electrons in AES. These σ_i values would not be directly useful in predicting the yield of ions from gas-phase samples as account would have to be taken of the cross sections for excitation of an inner-shell electron to unoccupied discrete states (although such cross sections would be expected to be small compared to σ_i; Dehmer and Saxon, 1973; Codling, 1973; Azaroff and Pease, 1974) and of the production of multiply charged ions in actual ion-yield measurements (Carlson *et al.*, 1966). Also, the cross sections to be discussed here refer exclusively to the production of *single* vacancies in a

* Work carried out at the U. S. National Bureau of Standards under the partial sponsorship of the U. S. Energy Research and Development Administration, Division of Biomedical and Environmental Research.

[1] It should be made clear that EPMA and AES are analytical techniques with different capabilities. One important difference is that in EPMA a surface region of depth about 1 μm is sampled (Goldstein, 1974) whereas in AES the corresponding depth is often between 3 and 30 Å (Powell, 1974).

particular atom; no consideration is given to the simultaneous production of multiple vacancies in a single ionizing collision (Carlson, *et al.*, 1970).

The main objective of this review is to determine a sound basis on which inner-shell ionization cross sections can be predicted for incident electron energies in the range of interest to EPMA and to AES. We are interested in the shape as well as the magnitude of the σ_i versus incident electron energy E_0 curve in order to ascertain whether data for one element can be scaled to apply to another. Owing to the shortage of data, it will be assumed that σ_i does not depend on phase or chemical composition although it is known that $d\sigma_i/dE$, the differential cross section with respect to excitation energy E, can differ for an element in the solid and gaseous phases and for an element in different compounds (for excitation energies near threshold); this point will be discussed later in Sec. IX. Also, the analysis of data will be limited to K-shell and L-shell ionization as very little data now exist for other shells.

It will be convenient to compare data with the use of the Bethe (1930) expression for inner-shell ionization. This choice has been made as the Bethe result has been frequently used in EPMA and as similar expressions due to Bethe have been extensively and successfully used to describe valence-shell excitation and ionization for atoms (Inokuti, 1971; Inokuti *et al.*, 1975). Much of the available inner-shell cross-section data is for incident electron energies less than 10 keV so that nonrelativistic formulas for data analysis should be satisfactory. The same formulas have been used here with some data obtained for electrons of higher energy as the nonrelativistic Bethe formula has been used extensively in EPMA and it was desired to determine optimum choices for the various parameters in a simple analytic formula.

The Bethe theory is described briefly in the following section. In Sec. III other quantum-mechanical theories are reviewed and values of "effective Bethe parameters" are derived. A similar procedure is followed in Sec. IV, where the available experimental data is reviewed and analyzed. We will briefly describe classical theories and semiempirical formulas for inner-shell ionization in Secs. V and VI, respectively. The various expressions for ionization cross sections and the results of the experimental measurements will be intercompared in Sec. VII. Information concerning one of the Bethe parameters can be derived from photoabsorption measurements, and the results of this analysis will be presented in Sec. VIII. Finally, in Sec. IX, we will attempt to assess the physical significance of the derived Bethe parameters and the extent to which they can be used to predict ionization cross sections in other materials.

II. THE BETHE THEORY OF INNER-SHELL IONIZATION

Bethe (1930) has expressed the cross section, per atom, for ionization of the nl shell in the form

$$\sigma_{nl}=\frac{2\pi e^4}{mv^2E_{nl}}Z_{nl}b_{nl}\ln\left[\frac{2mv^2}{B_{nl}}\right], \tag{1}$$

where $E_0=\frac{1}{2}mv^2$ is the energy of the incident electron beam, E_{nl} is the binding energy of electrons in the nl shell, and Z_{nl} is the number of electrons in that shell. The parameter b_{nl} was estimated by Bethe (using hydrogenic wave functions) to be between 0.2 and 0.6 for inner shells and, for a given shell, to be a function of Z. The energy B_{nl} was estimated by Bethe to be of the order of E_{nl}. Equation (1) was derived with the use of the first Born approximation and is expected to be valid when E_0 is much greater than E_{nl} and when the energy transfer in the ionizing collision is much less than E_0 (Inokuti, 1971; Cooper, 1973). The question then arises as to how much greater E_0 should be than E_{nl}; this problem will be discussed in Sec. IX.

With values of the constants inserted, Eq. (1) becomes

$$\sigma_{nl}=\frac{6.51\times10^{-14}}{E_0E_{nl}}Z_{nl}b_{nl}\ln\left[\frac{c_{nl}E_0}{E_{nl}}\right]\ \text{cm}^2, \tag{2}$$

where $c_{nl}=4E_{nl}/B_{nl}$ and where the energies E_0 and E_{nl} have been expressed in electron volts. It is convenient to rewrite Eq. (2) in terms of the dimensionless variable $U_{nl}=E_0/E_{nl}$ to permit easy comparisons of cross sections for different elements:

$$\sigma_{nl}E_{nl}^2=6.51\times10^{-14}Z_{nl}b_{nl}\ln[c_{nl}U_{nl}]/U_{nl}\ \text{cm}^2\cdot\text{eV}^2. \tag{3}$$

In the remainder of this paper we will attempt to find optimum choices for the Bethe parameters b_{nl} and c_{nl} in Eqs. (2) and (3). More specific calculations for particular atoms will be compared with Eq. (3) and used, where appropriate, to determine b_{nl} and c_{nl}. We will also intercompare experimental ionization cross-section data on the basis of Eq. (3) and similarly derive effective values of the Bethe parameters. These parameters can be obtained conveniently from a linear least-squares fit to the following equation (a Fano plot):

$$\frac{\sigma_{nl}E_{nl}^2U_{nl}}{6.51\times10^{-14}Z_{nl}}=b_{nl}\ln U_{nl}+A_{nl}, \tag{4}$$

where $A_{nl}=b_{nl}\ln c_{nl}$; that is, from a plot of the left-hand side of Eq. (4) versus $\ln U_{nl}$ (Fano, 1954; Schram *et al.*, 1965; Schram and Vriens, 1965; Inokuti, 1971). A plot of this type also reveals the minimum energy for which Eqs. (1)–(3) are valid.

III. OTHER QUANTUM-MECHANICAL CALCULATIONS OF INNER-SHELL IONIZATION CROSS SECTIONS

Madison and Merzbacher (1975) have reviewed theories of K-shell ionization by electrons with emphasis on calculations and data at high electron energies for medium-Z and high-Z atoms, where relativistic effects are important. As pointed out earlier, we will emphasize cross-section formulas for low electron energies, where nonrelativistic formulas are useful.

Burhop (1940) has computed cross sections for the removal (i.e., true ionization) of K-shell electrons from atomic Ni, Ag, and Hg, and of L_1-, L_2-, and L_3-shell electrons from atomic Ag and Hg. Burhop's formula has also been evaluated recently by Hink *et al.* (1969) for the case of removal of K-shell electrons from Be, Al, and Ni; only a slight variation of the values of $\sigma_KE_K^2$ with Z was found. The cross-section data of Burhop have been analyzed by Mott and Massey (1949), who concluded that,

if the contributions to σ_{nl} due to transitions to unoccupied discrete levels could be neglected, a reasonable approximation (Dehmer and Saxon, 1973; Codling, 1973; Azaroff and Pease, 1974), then $b_K \approx 0.35$, $b_L \approx 0.25$, and $c_K = c_L \approx 2.42$ (corresponding to $B_{nl} = 1.65E_{nl}$ for both K- and L-shell ionization). Figure 1(a) shows a plot of $\sigma_K E_K^2$ versus U_K [Eq. (3)] with the Mott and Massey values for b_K and c_K; a similar plot of Burhop's values of $\sigma_K E_K^2$ for Ni is shown in Fig. 1(b).

The Bethe parameters derived by Mott and Massey (1949) have been widely used in model calculations and correction procedures for the electron-probe microanalyzer. A least-squares fit to the Burhop data [using Eq. (4)], however, yielded substantially different values of b_{nl} and c_{nl}, as shown in Tables I and II, from those derived by Mott and Massey.

Equations (1)–(3) are not valid at low energies and do not therefore show a realistic dependence of σ_{nl} on E_0 near threshold ($U_{nl} = 1$). Worthington and Tomlin (1956) arbitrarily modified the logarithmic term in the Bethe equation to give a plausible representation of the ionization cross section near threshold. Their modification of Eq. (3) is

$$\sigma_{nl}E_{nl}^2 = \frac{6.51\times10^{-14}Z_{nl}b_{nl}}{U_{nl}} \times\ln\left[\frac{4U_{nl}}{1.65+2.35\exp(1-U_{nl})}\right] \text{ cm}^2\cdot\text{eV}^2 . \quad (5)$$

For large U, Eq. (5) becomes identical to Eq. (3) (with $c_{nl} = 2.42$). Figures 1(a) and 2(a) show plots of Eq. (5) near threshold for K- and L-shell ionization where again the Mott and Massey values of b_{nl} have been used.

Arthurs and Moiseiwitsch (1958) have computed an expression for true K-shell ionization from atoms using Moller's relativistic modification of the Born approximation; this expression should be valid for $Z < 30$. Their equation has been evaluated for Al and Ni and plotted in Fig. 1(b). The computed values have also been fitted to Eq. (4) and the derived Bethe parameters are shown in Table I. Perlman (1960) extended the work of Arthurs and Moiseiwitsch to heavier atoms. His computed cross-section curve for Ni is shown in Fig. 1(b) and the derived Bethe parameters are given in Table I. Perlman's result for Ni does not differ appreciably from that of Arthurs and Moiseiwitsch.

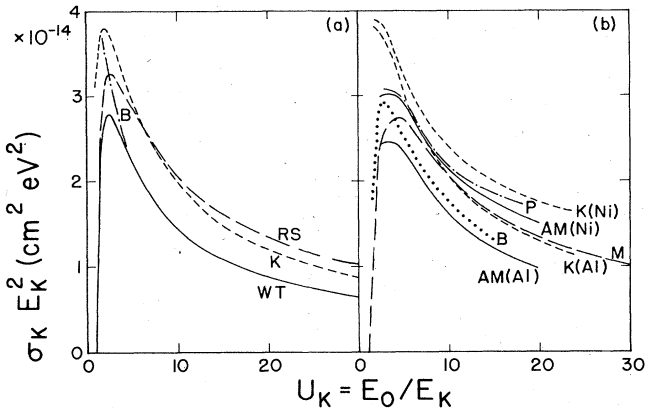

FIG. 1. Plots of $\sigma_K E_K^2$ versus U_K. (a) The dot–dash line denoted B is the Bethe (1930) equation [Eq. (3)] with $b_K = 0.35$ and $c_K = 2.42$; the solid line denoted WT is the Worthington–Tomlin (1956) equation [Eq. (5)] with $b_K = 0.35$; the long-dashed line denoted RS is the Rudge and Schwartz (1966) result [Eqs. (6) and (7a)]; and the short-dashed curve denoted K is Kolbenstvedt's (1967) result [Eq. (8)]. (b) The dotted curve denoted B is Burhop's (1940) result for Ni; the solid lines denoted AM are the results of Arthurs and Moiseiwitsch (1958) for Al and Ni; the short-dashed lines denoted K are Kolbenstvedt's (1967) results for Al and Ni; the dot–dashed line denoted P is Perlman's (1960) result for Ni; and the long-dashed curve denoted M is McGuire's (1971a, 1974) results for Be, C, and O.

Rudge and Schwartz (1966) have computed K-shell and L_1-shell ionization cross sections for atomic hydrogen, He^+, and a fictitious hydrogenic ion with $Z = 128$. Their results can be expressed in the form

$$\sigma_{nl}E_{nl}^2 = 1.626\times10^{-14}Z_{nl}Q_{nl}(U_{nl}) \text{ cm}^2\cdot\text{eV}^2 . \quad (6)$$

The term $Q_{nl}(U_{nl})$ is a reduced cross section that has been calculated in the second-Born and Born-exchange approximations and found to be weakly dependent on Z. As pointed out by Hink and Ziegler (1969), the change in $Q_{nl}(U_{nl})$ on going from $Z = 2$ to $Z = 128$ is smaller than the change on going from $Z = 1$ to $Z = 2$. We therefore quote the results for $Z = 128$,

$$Q_K(U_K) = \frac{\ln U_K}{U_K}\left[2.799 - \frac{0.218}{U_K} + \frac{0.047}{U_K^2}\right] \quad (7a)$$

and

$$Q_{L_1}(U_{L_1}) = \frac{\ln U_{L_1}}{U_{L_1}}\left[2.168 + \frac{1.147}{U_{L_1}} - \frac{0.212}{U_{L_1}^2}\right], \quad (7b)$$

which have been obtained from calculations of $Q_{nl}(U_{nl})$ for U_{nl} between 1.25 and 4. We have arbitrarily assumed that Eq. (7) is useful for larger values of U_{nl}. Computed values of $\sigma_K E_K^2$ and $\sigma_{L_1}E_{L_1}^2$ have been used to derive the Bethe parameters shown in Tables I and II; $\sigma_K E_K^2$ is also plotted in Fig. 1(a) and is seen to be considerably larger than the values obtained using Eq. (3) with the Mott and Massey parameters.

Kolbenstvedt (1967) has derived a relatively simple approximate formula for K-shell ionization applicable to relativistic electrons and heavy atoms. His result can be simplified for nonrelativistic energies to become

$$\sigma_K E_K^2 = \frac{3.590\times10^{-14}\ln(2.38U_K)}{U_K} + \frac{1.293\times10^{-13}}{U_K}\left[1 - \frac{(1+\ln U_K)}{U_K}\right] \text{ cm}^2\cdot\text{eV}^2 \quad (8)$$

and is plotted in Fig. 1(a). The relativistic expression has also been evaluated for Al and Ni and the result is shown in Fig. 1(b).

McGuire (1971a, 1971b, 1974) has computed generalized oscillator strengths (Bethe, 1930; Inokuti, 1971) for the various subshells of low-Z atoms from which he has derived the corresponding ionization cross sections. His results of $\sigma_K E_K^2$ versus U_K for Be, C, and O lie on a smooth curve, indicated in Fig. 1(b), but the values for Ne lie about 10% higher; the data for F is intermediate. It is clear from the results of Arthurs and Moiseiwitsch, Kolbenstvedt, and McGuire that there is a

TABLE I. Values of Bethe parameters b_K and c_K and their probable errors obtained from the linear least-squares fits (described in Sec. II) to calculated K-shell ionization cross sections for the range of U_K indicated.

Author	Element	Range of U_K	b_K	c_K
Burhop (1940)	Ni	4–15	0.50 ± 0.01	1.41 ± 0.08
	Ag	3–7	0.70 ± 0.01	0.92 ± 0.03
	Hg	3–10	0.70 ± 0.02	1.16 ± 0.07
Arthurs and Moiseiwitsch (1958)	Ni	5–20	0.88 ± 0.03	0.70 ± 0.07
	Al	5–20	0.42 ± 0.02	1.91 ± 0.28
Perlman (1960)	Ni	3–18	0.93 ± 0.04	0.68 ± 0.07
Rudge and Schwartz (1966)		7–50	0.700 ± 0.001	0.965 ± 0.001
Kolbenstvedt (1967)		5–40	0.46 ± 0.01	2.62 ± 0.23
McGuire (1971a, 1974)	Be	5.8–62	0.66 ± 0.01	1.10 ± 0.06
	C	5.8–25	0.71 ± 0.01	0.95 ± 0.03
	O	6.1–23	0.73 ± 0.01	0.91 ± 0.01
	Ne	7–15	0.76 ± 0.01	1.04 ± 0.03
	Be, C, O	5.8–62	0.68 ± 0.01	1.06 ± 0.03
Gryzinski (1965)		10–30	0.54 ± 0.01	1.86 ± 0.16
Drawin (1961, 1963)		5–30	0.756 ± 0.003	0.73 ± 0.01
Lotz (1970)		10–30	0.62 ± 0.001	0.99 ± 0.01

rise in $\sigma_K E_K^2$ as Z is increased from 10 to 28. This factor has to be kept in mind when intercomparing the theoretical results and when comparing theory with experiment. Specifically, the nonrelativistic formulas should be compared with experimental cross-section data only when $E_K \lesssim 1$ keV and when $E_0 \lesssim 10$ keV.

McGuire (1971a, 1974) has also calculated L_1, L_{23}, and M_1-shell ionization cross sections for $Z < 18$ (Ar). His values of $\sigma_{L_{23}} E_{L_{23}}^2$ for Na, Al, S, and Ar are plotted as a function of $U_{L_{23}} = E_0/E_{L_{23}}$ in Fig. 2(b) and it is seen that there is a substantial variation from element to element. McGuire has found empirically that values of $\sigma_{L_{23}} E_{L_{23}}^{\epsilon}$ for Na through Ar plotted as a function of $U_{L_{23}}$ lie close to a common curve for $U_{L_{23}} \gtrsim 10$ and $\epsilon = 1.62$.

We have fitted McGuire's cross-section data to Eq. (4) and the resulting values of the Bethe parameters are shown in Tables I and II. Values of $b_{L_{23}}$ and $c_{L_{23}}$ are plotted as a function of $E_{L_{23}}$ on logarithmic scales in Fig. 3. Straight-line least-squares fits to the relations

$$\log b_{L_{23}} = \alpha \log E_{L_{23}} + \beta$$

and

$$\log c_{L_{23}} = \gamma \log E_{L_{23}} + \delta$$

have been made to yield the parameters $\alpha = 0.30 \pm 0.01$, $\beta = -0.74 \pm 0.02$, $\gamma = 0.22 \pm 0.03$, and $\delta = -0.58 \pm 0.07$.

Manson (1972, 1974) has computed L_1- and L_{23}-shell ionization cross sections for Al using a model similar to that of McGuire for incident electron energies of 2, 3, and 4 keV. His results have been fitted to Eq. (4) and the Bethe parameters are shown in Table II. The value of $\sigma_{L_{23}} E_{L_{23}}^2$ for $E_0 = 2$ keV is shown in Fig. 2(b) and corresponds closely to McGuire's result for Al.

Wallace, Berg, and Green (1973) have evaluated gen-

TABLE II. Values of Bethe parameters b_L and c_L and their probable errors obtained from the linear least-squares fits to calculated L-shell ionization cross sections for the range of U_L indicated.

Author	Element	Subshell	Range of U_L	b_L	c_L
Burhop (1940)	Ag	L_1	3–15	0.31 ± 0.02	1.72 ± 0.26
		L_2	3–15	0.29 ± 0.02	2.04 ± 0.46
		L_3	3–15	0.28 ± 0.02	1.86 ± 0.30
	Hg	L_1	3–15	0.35 ± 0.02	2.36 ± 0.54
		L_2	3–15	0.36 ± 0.02	1.91 ± 0.32
		L_3	3–15	0.32 ± 0.02	1.85 ± 0.33
Rudge and Schwartz (1966)		L_1	7–50	0.513 ± 0.001	1.29 ± 0.01
McGuire (1974)	Na	L_{23}	9–88	0.52 ± 0.02	0.59 ± 0.08
	Al	L_{23}	5–94	0.67 ± 0.01	0.61 ± 0.03
	Si	L_{23}	6–80	0.71 ± 0.01	0.71 ± 0.03
	S	L_{23}	6–48	0.87 ± 0.01	0.82 ± 0.03
	Cl	L_{23}	7–50	0.88 ± 0.01	0.95 ± 0.03
	Ar	L_{23}	5–30	0.98 ± 0.01	0.82 ± 0.02
Manson (1974)	Al	L_1	17–34	0.32 ± 0.01	8.8 ± 1.0
		L_{23}	27–55	0.60 ± 0.01	1.70 ± 0.01
Wallace *et al.* (1973)	Ar	L_1	9–31	3.5 ± 0.1	0.22 ± 0.03
		L_{23}	8–41	2.40 ± 0.01	0.33 ± 0.03
Lotz (1970)		L_{23}	10–30	0.54 ± 0.01	0.48 ± 0.04

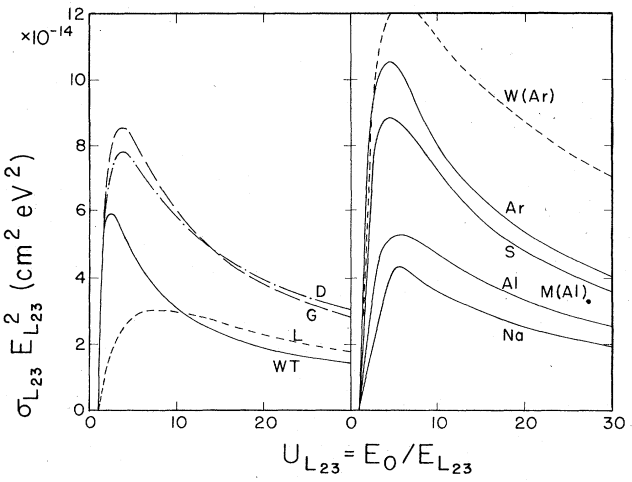

FIG. 2. Plots of $\sigma_{L_{23}}E_{L_{23}}^2$ versus $U_{L_{23}}$. (a) The solid line denoted WT is the Worthington–Tomlin (1956) equation [Eq. (5)] with $b_L = 0.25$; the long-dashed line denoted G is the Gryzinski (1965) expression [Eq. (9)]; the dot–dashed line denoted D is the Drawin (1961, 1963) result [Eq. (10)]; and the short-dashed line denoted L is the Lotz (1970) expression [Eq. (11)] with $a_{L_{23}} = 2.6\times10^{-14}$ cm$^2\cdot$eV^2, $b_{L_{23}} = 0.92$, and $c_{L_{23}} = 0.19$. (b) The solid lines are McGuire's (1974) results for Na, Al, S, and Ar; the short-dashed line denoted W(Ar) is the result of Wallace *et al.* (1973) for Ar; and the point denoted M(Al) is Manson's (1972, 1974) result for Al.

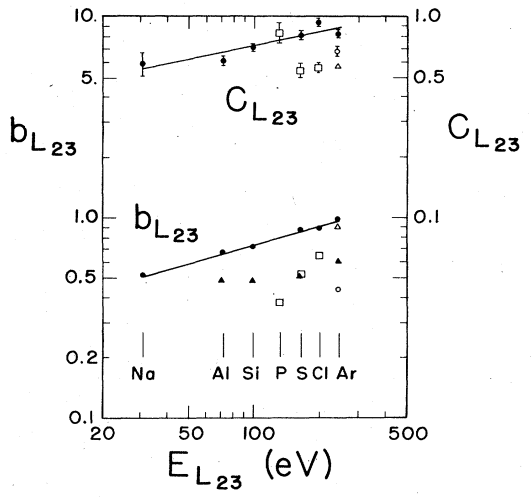

FIG. 3. Plots of $b_{L_{23}}$ and $c_{L_{23}}$ (solid circles) derived from the fits to Eq. (4) using McGuire's (1974) calculated cross sections for Na, Al, Si, S, Cl, and Ar (Table II) as a function of $E_{L_{23}}$. The open symbols are values of $b_{L_{23}}$ and $c_{L_{23}}$ derived from the fits to experimental cross sections (Table IV) for P, S, and Cl (open squares, data of Vrakking and Meyer, 1974), for Ar (open circles, data of Ogurtsov, 1973) and for Ar (open triangles, data of Christofzik, 1970). The solid triangles are values of $b_{L_{23}}$ estimated from photoabsorption data (Sec. VIII).

eralized oscillator strengths for Ar from which they derive cross sections for ionization of the L_1 and L_{23} subshells. Values of $\sigma_{L_{23}}E_{L_{23}}^2$ obtained from their calculations are shown in Fig. 2(b), and it can be seen that their values are considerably greater than those of McGuire for Ar.

IV. MEASUREMENTS OF INNER-SHELL IONIZATION CROSS SECTIONS

Three techniques have been used to make the limited number of inner-shell ionization cross-section measurements that now exist. The earliest measurements were made by measuring the absolute yield of characteristic x rays emitted from a solid target bombarded by electrons (Webster *et al.*, 1933). One important parameter that is needed in these measurements is the fluorescent yield. For inner-shell vacancies caused by the removal of core electrons of low binding energy ($\lesssim$1 keV), the fluorescent yield is low ($\lesssim$0.01) and often poorly known (Bambynek *et al.*, 1972) so that the derived ionization cross sections in the range of interest to AES can have large uncertainties. This difficulty can be overcome by measuring instead the total yield of characteristic Auger electrons corresponding to all decay channels of a particular inner-shell vacancy (Glupe and Mehlhorn, 1967). A third method of determining inner-shell ionization cross sections is from measurements of the energy-loss spectra of electrons transmitted through thin target films (Swanson and Powell, 1968). The total intensity of features associated with excitation of electrons from a particular inner shell needs to be measured, but this quantity may not be measurable if there is significant overlap of intensities for excitation from other shells.

Measurements of the absolute yield of $K\alpha$ x rays from thin targets of Ni ($U_K = 8.3$ keV) have been used to derive K-shell ionization cross sections as a function of electron energy (Smick and Kirkpatrick, 1945; Pockman *et al.*, 1947). These measurements are shown in Fig. 4(a) and a Fano plot of this data in the form indicated by Eq. (4) is given in Fig. 5. The derived Bethe parameters b_K and c_K are listed in Table III.

Other measurements of the same type (Webster *et al.*, 1933; Clark, 1935; Hansen *et al.*, 1964; Motz and Placious, 1964; Hansen and Flammersfeld, 1966; Rester

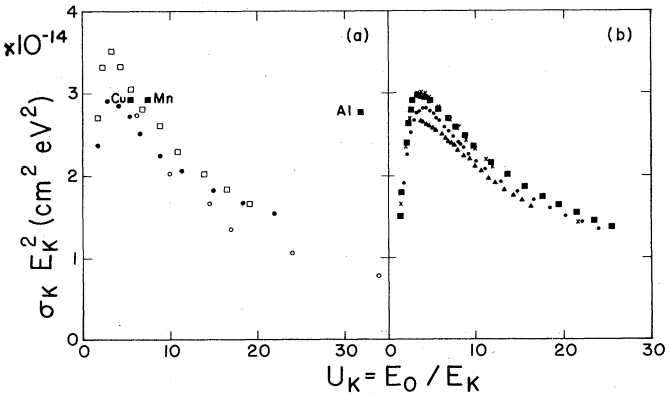

FIG. 4. Experimental values of $\sigma_K E_K^2$ as a function of U_K. (a) Solid circles denote data of Pockman *et al.* (1947) for Ni; solid squares denote data of Fischer and Hoffman (1967) for Al, Mn, and Cu; the open squares denote the results of Hink and Ziegler (1969) for Al; and the open circles denote the results of Hink and Paschke (1971a, 1971b) for C. (b) Results of Glupe and Mehlhorn (1967, 1971), of Glupe (1972), and of Bekk (1974) for C (triangles), Ne (crosses), N (squares), and O (circles).

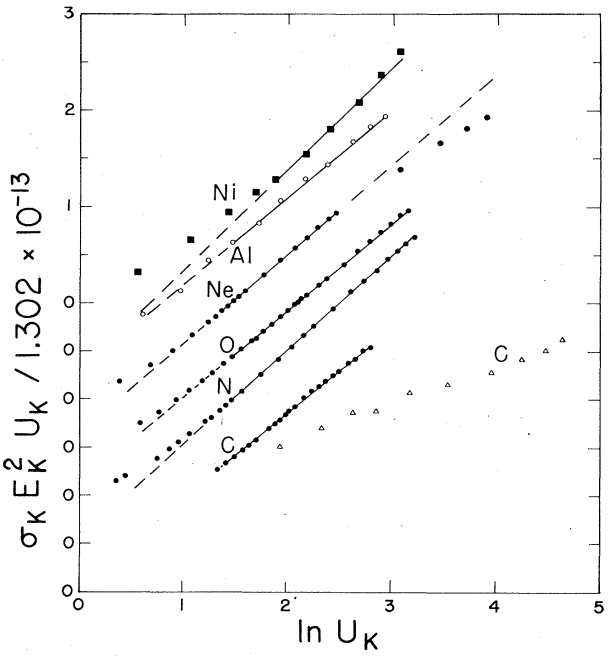

FIG. 5. Plot of experimental values of $\sigma_K E_K^2 U_K / 1.302 \times 10^{-13}$ [left-hand side of Eq. (4)] versus $\ln U_K$. The solid squares are the data of Pockman *et al.* (1947) for Ni; the open circles are the data of Hink and Ziegler (1969) for Al; the solid circles are the data of Glupe and Mehlhorn (1967, 1971), of Glupe (1972), and of Bekk (1974) for C, N, O, and Ne; and the open triangles are the data of Hink and Paschke (1971a, 1971b) for C. Successive plots have been displaced vertically for clarity. The solid lines represent the least-squares fits of each set of data to Eq. (4) with the derived Bethe parameters shown in Table III for the range of U_K indicated; the dashed portions of each line represent extrapolations.

and Dance, 1966; Davis *et al.*, 1972; Dangerfield and Spicer, 1975) have been made for larger values of U_K (higher Z) but will not be discussed here as appreciable relativistic corrections appear to be necessary in the theory (Madison and Merzbacher, 1975) and become necessary in the formulas. Fischer and Hoffmann (1967) determined K-shell ionization cross sections from measured x-ray yields for electrons of a fixed energy (50 keV) bombarding Al, Mn, Cu, Se, Ag, and Sn. Their results (for which there is an uncertainty of about 50%) for Al, Mn, and Cu are shown in Fig. 4(a). Green and Cosslett (1968) measured L_2- and L_3-shell ionization cross sections of Au for low values of $U_{L_{23}}$ (≤ 3.3); these cross sections were appreciably higher (by about 30% to 100%, depending on the values selected for the fluorescence yield) than expected from Burhop's (1940) calculations.

Inner-shell ionization cross sections have also been derived from measurements of the yield of characteristic x rays emitted from thick targets under electron bombardment. Hink (1964, 1965) has reported values of σ_K and σ_{L_3} for Cu and W, respectively, for low values of U_{nl} (<4). These measurements indicated appreciably higher values of b_{nl} than those recommended by Mott and Massey (1949) although it would not be expected that Eqs. (1) to (3) would be valid for such low values of U_{nl}. Similar measurements for larger values of U_{nl} have been reported for Al and C by Hink and co-workers (Hink and Ziegler, 1969; Hink and Paschke, 1971a, 1971b) and these are shown in Figs. 4(a) and 5. The Fano plot for Al in Fig. 5 is linear but, as noted by Tawara *et al.* (1973), the Fano plot for C is not. It would therefore appear that there is an energy-dependent systematic error in the cross-section data for carbon.

Fong and Tomlin (1970) have concluded from their own and other measurements of x-ray yields that Burhop's (1940) calculations underestimate σ_L by a factor of about 2. A similar conclusion was reached by Brown and Gilfrich (1971), who compared measured $K\alpha$ and $L\alpha$ intensities with those expected from an electron-transport calculation. These authors also found that Burhop's calculated K-shell ionization cross sections should be increased by 20% to make the calculated x-ray yields agree reasonably with experiment.

We now turn to ionization cross sections determined from yields of characteristic Auger electrons. Glupe and Mehlhorn (1967, 1971) and Glupe (1972) have measured σ_K for C, N, O, and Ne and their results are shown in Fig. 4(b) and the corresponding Fano plots in Fig. 5. Gaseous samples were used (C in CH_4) so no corrections for electron scattering in the sample of the type required for solids were necessary. Further measurements of σ_K for Ne have been made by Bekk (1974) and of $\sigma_{L_{23}}$ for Ar by Christofzik (1970); these measurements are shown in Figs. 4(b), 5, 6, and 7.

The same technique has been used by several other authors. Meyer and Vrakking (1973) and Vrakking and Meyer (1974) have measured $\sigma_{L_{23}}$ for Si, P, S, Cl, Ti, Br, and Sn in molecules containing these elements and C or Cl. All Auger-electron yields were measured rela-

TABLE III. Values of Bethe parameters b_K and c_K and their probable errors obtained from the linear least-squares fits to measured K-shell ionization cross sections for the range of U_K indicated.

Author	Element	Range of U_K	b_K	c_K
Pockman *et al.* (1947)	Ni	5.5–22	1.05 ± 0.03	0.51 ± 0.05
Hink and Ziegler (1969)	Al	4.4–19.2	0.90 ± 0.01	0.79 ± 0.02
Glupe and Mehlhorn (1967, 1971) and Glupe (1972)	C	4.2–16.4	0.887 ± 0.004	0.62 ± 0.01
	N	4.4–25.5	0.970 ± 0.004	0.63 ± 0.01
	O	4.3–23.9	0.908 ± 0.003	0.63 ± 0.01
	Ne	4–12	0.932 ± 0.003	0.67 ± 0.01

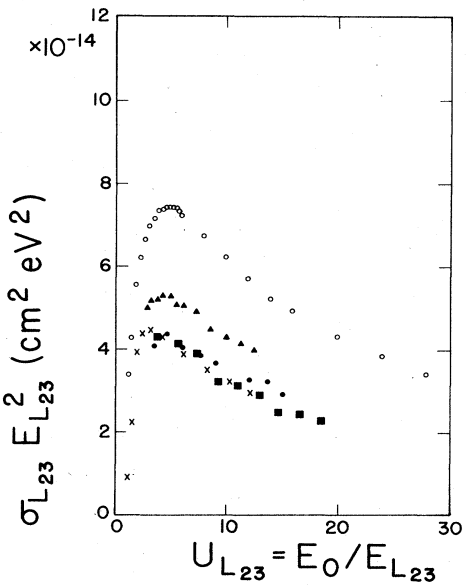

FIG. 6. Experimental values of $\sigma_{L_{23}}E^2_{L_{23}}$ as a function of $U_{L_{23}}$. The solid symbols are the data of Vrakking and Meyer (1974) for P (squares), S (circles), and Cl (triangles); the crosses are the data of Ogurtsov (1973) for Ar; and the open circles are the data of Christofzik (1970) for Ar.

tive to those for C and the absolute cross sections were obtained by reference to Glupe and Mehlhorn's (1967, 1971) measurements of σ_K for C. Values of $\sigma_{L_{23}}$ were obtained over a significant range of $U_{L_{23}}$ only for P, S, and Cl and these results are shown in Figs. 6 and 7. Vrakking and Meyer assumed that the cross-section curves as a function of $U_{L_{23}}$ for the other elements had the same shape as that of S, P, and Cl and thus estimated the peak ionization cross section (at $U_{L_{23}}=4$) where it could not be measured. Values of the maximum cross section were found to fit the empirical relation $\sigma_{L_{23}}(U_{L_{23}}=4) = 4.98\times10^{-15}E_{L_{23}}^{-1.56}\,\mathrm{cm}^2$ (with $E_{L_{23}}$ in eV). Ogurtsov (1973) has determined $\sigma_{L_{23}}$ for Ar from measured yields of Auger electrons and his results are shown in Figs. 6 and 7.

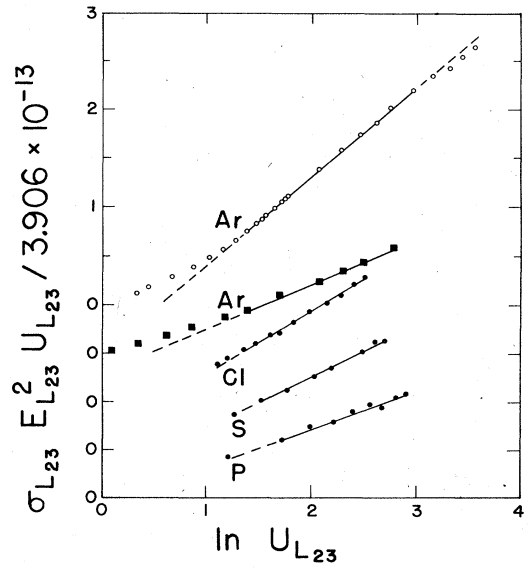

FIG. 7. Plot of experimental values of $\sigma_{L_{23}}E^2_{L_{23}}U_{L_{23}}/3.906\times10^{-13}$ [left-hand side of Eq. (4)] versus $\ln U_{L_{23}}$. The solid circles are the data of Vrakking and Meyer (1974) for P, S, and Cl, the squares are the data of Ogurtsov (1973) for Ar, and the open circles are the data of Christofzik (1970) for Ar. The solid lines represent least-squares fits of each set of data to Eq. (4) with the derived Bethe parameters shown in Table IV for the range of $U_{L_{23}}$ indicated; the dashed portions of each line represent extrapolations. Successive plots have been displaced vertically for clarity.

Gerlach and DuCharme (1972) and DuCharme and Gerlach (1973) derived ionization cross sections from Auger-electron yields of atoms adsorbed on surfaces for low values of U_{nl} (<6) but as their values are uncertain by a factor between 2 and 4 (due to uncertainties in surface coverage) the results are not shown here. Powell *et al.* (1975) have reported results of a preliminary experiment in which ionization cross sections could be obtained from the yield of Auger electrons emitted from solid samples. This method, based on the use of a simple model for the transport of the Auger electrons in the sample and on knowledge of the inelastic attenuation length at the Auger-electron energy, was used to derive values of $\sigma_{L_{23}}$ for Al in the range $27 < U_{L_{23}} < 41$; these values are considered approximate on account of assumptions made in the analysis. Finally, Gallon (1972) has developed an iterative method for determining inner-shell ionization cross sections from measured Auger-electron yields in a typical AES experiment. So far, only relative data (that is, the shape of the cross-section curve versus incident electron energy) have been determined (Gallon, 1972; Smith and Gallon, 1974).

We now summarize measurements of inner-shell ionization cross sections derived from transmission electron energy-loss experiments. A single primary-electron energy has been used in some of the measurements made to date so that in these cases it is possible to determine b_{nl} only if a value is assumed for c_{nl}. Swanson and Powell (1968) determined $b_L=0.55$ for Al with $c_L=4$ using 20 keV incident electrons ($U_L=241$); this value of b_L, which has an estimated uncertainty of ±40%, was derived from intensity measurements over a small range of excitation energies so it should be regarded as a lower limit (see also Sec. IX below). A value of $b_K=0.14$ (with $c_K=4$) was derived from a K-shell ionization cross section for carbon obtained by Colliex and Jouffrey (1972) with 75 keV electrons ($U_K=264$); the range of integration of energy loss was not specified so this determination should also be considered as a lower limit. Isaacson (1972) has measured K-shell ionization cross sections with 25 keV electrons for C, N, and O in nucleic-acid bases from which values of $b_K=0.70$, 0.74, and 0.78, respectively, have been determined (with an uncertainty of about ±25%). These values (for which $c_K=4$) should be regarded as lower limits to the true values of b_K on account of the limited range of scattering angles accepted in the experiment. Egerton (1975) has performed a similar energy-loss experiment with 80 keV electrons incident on amorphous carbon ($U_K=282$) from which a value of $b_K=0.9$ with an uncertainty of about ±10% has been obtained.

V. CLASSICAL THEORIES OF INNER-SHELL IONIZATION

A number of reviews dealing with early and recent classical theories of ionization have appeared recently (Peterkop and Veldre, 1966; Burgess and Percival, 1968; Vriens, 1969). The theory that has appeared to be the most successful is that of Gryzinski (1965). His result for the ionization cross section can be expressed in the form

$$\sigma_{nl}E_{nl}^2 = 6.51\times10^{-14}Z_{nl}g(U_{nl})\ \text{cm}^2\cdot\text{eV}^2, \tag{9a}$$

where

$$g(U_{nl}) = \frac{1}{U}\left(\frac{U-1}{U+1}\right)^{3/2}\left[1+\frac{2}{3}\left(1-\frac{1}{2U}\right)\ln[2.7+(U-1)^{1/2}]\right]. \tag{9b}$$

Equation (9) is plotted in Figs. 8 and 2(a) for K- and L_{23}-shell ionization, respectively. The computed values have been fitted to the Bethe cross section [Eq. (4)] and the derived parameters are shown in Table I.

VI. SEMIEMPIRICAL FORMULAS FOR INNER-SHELL IONIZATION

Drawin (1961, 1963) has summarized various early semiempirical formulas used to describe cross sections for ionization. He also has proposed the following formula:

$$\sigma_{nl}E_{nl}^2 = 4.32\times10^{-14}Z_{nl}f_1(U_{nl}-1)\times\ln(1.25f_2U_{nl})/U_{nl}^2\ \text{cm}^2\cdot\text{eV}^2, \tag{10}$$

where f_1 and f_2 are parameters estimated to have values in the ranges 0.7–1.3 and 0.8–3.0, respectively, but which are often assumed to be unity. For $U_{nl}\gg1$, Eq. (10) reduces to Eq. (3) with $b_{nl}=0.66$ and $c_{nl}=1.25$. For $5<U_{nl}<30$, values of $\sigma_{nl}E_{nl}^2$ have been fitted to Eq. (4) and the derived Bethe parameters are shown in Table I. Equation (10) is plotted in Figs. 2(a) and 8.

Lotz (1967, 1968, 1969, 1970) has proposed the formula

$$\sigma_{nl}E_{nl}^2 = a_{nl}Z_{nl}\ln U_{nl}\{1-b_{nl}\exp[-c_{nl}(U_{nl}-1)]\}/U_{nl} \tag{11}$$

and has assigned best values to the three parameters a_{nl}, b_{nl}, and c_{nl} [which should not be confused with the Bethe parameters in Eq. (3)]. Equation (11) is plotted in Figs. 2(a) and 8 for ionization of the K and L_{23} shells and values of the derived Bethe values are shown in Tables I and II; computed cross sections for ionization of the L_1 shell are essentially identical (within 6%) to those of the K shell for $U\geq5$. The parameter values were selected by Lotz so that Eq. (11) could describe cross sections for the removal of outer-shell electrons from atoms to produce ions. Pessa and Newell (1971) have subsequently assumed that a slightly simplified version of Eq. (11) can be used to predict cross sections for the production of vacancies in inner shells (in the range of interest for EPMA and AES).

Equation (11) reduces to Eq. (3) for large U_{nl} if c_{nl} in Eq. (3) is close to unity. Green and Cosslett (1961) assumed for simplicity that $c_K=1$ in Eq. (3) and put $b_K=0.61$ to agree with experimental data for Ni and Ag at $U_K=3$. They have then used their modified Eq. (3) and a similar approximation for L-shell ionization [using Burhop's (1940) calculated cross sections for normalization] in an analysis to predict the efficiency of production of characteristic x rays in the electron-probe microanalyzer (Green and Cosslett, 1968).

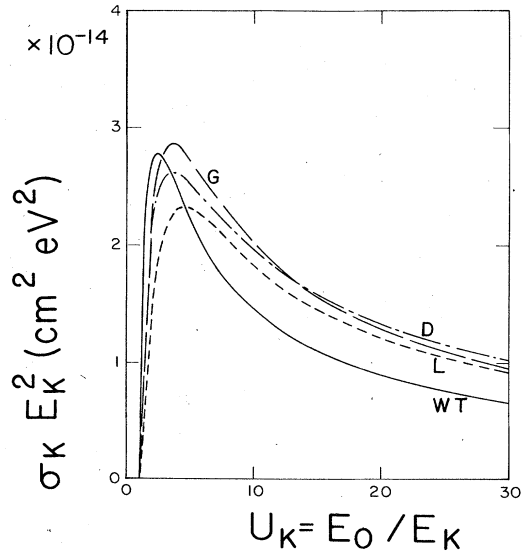

FIG. 8. Plots of $\sigma_K E_K^2$ versus U_K. The solid line denoted WT is the Worthington–Tomlin (1956) equation [Eq. (5)] with $b_K=0.35$; the long-dashed line denoted G is the Gryzinski (1965) expression [Eq. (9)]; the dot–dashed line denoted D is the Drawin (1961, 1963) result [Eq. (10)]; and the short-dashed line denoted L is the Lotz (1970) expression [Eq. (11)] with $a_K=4\times10^{-14}$ cm$^2\cdot$eV^2, $b_K=0.75$, and $c_K=0.5$.

VII. COMPARISON OF CROSS-SECTION THEORY AND MEASUREMENTS

We will now compare the results of the various calculations and measurements. Both the Bethe equation [Eq. (3)] and the Worthington–Tomlin equation [Eq. (5)] with $b_K=0.35$ as recommended by Mott and Massey (1949) lie systematically below the results of Kolbenstvedt [Eq. (8)] and of Rudge and Schwartz [Eqs. (6) and (7a)] shown in Fig. 1(a). The plots of $\sigma_K E_K^2$ in Fig. 1(b) from the work of Arthurs and Moiseiwitsch (1958) and of Kolbenstvedt (1967) show the rise with increasing Z referred to in Sec. III. The results of three relativistic calculations for nickel in Fig. 1(b) [those of Arthurs and Moiseiwitsch (1958), Perlman (1960), and Kolbenstvedt (1967)] are in moderate agreement with each other and with the experimental measurements of Kirkpatrick *et al.* shown in Fig. 4(a); these three calculations predict higher cross sections than the nonrelativistic calculation of Burhop (1940) also shown in Fig. 1(b). McGuire's (1971a, 1974) results for Be, C, and O shown in Fig. 1(b) agree closely with the results of Rudge and Schwartz (1966) in Fig. 1(a) except close to threshold (with $U_K\lesssim6$).

The widely used expressions of Gryzinski (1965), Drawin (1961), and Lotz (1970) for K-shell ionization are shown in Fig. 8 and agree closely with each other. These expressions also agree well (generally within about 10%) with the results of McGuire (1971a, 1974) shown in Fig.

1(b); similar agreement is found with the results of Rudge and Schwartz (1966) and of Kolbenstvedt (1967) in Fig. 1(a), except for the region near threshold with $U_K \lesssim 6$. Despite this apparent good agreement, there is a fairly large variation in the derived values of the Bethe parameters b_K and c_K shown in Table I. For example, values of b_K are 0.42 for Al from the work of Arthurs and Moiseiwitsch (1958), 0.46 from the result of Kolbenstvedt (1967), and 0.76 from Drawin's (1961) expression. Similar (inverse) variations are found for values of the parameter c_K; this is to be expected as b_K and c_K are fairly highly correlated [Eq. (4)]. Nevertheless, it has often been assumed that $B_K = E_K$ in Eq. (1) so that $c_K = 4$; a value $c_K \approx 4$ can in fact be inferred from the experiments of Egerton (1975) and of Severly *et al.* (1974). The values of c_K ranging from 0.73 to 2.62 in Table I are thus appreciably lower than expected. This apparent discrepancy is discussed further in Sec. IX.

It seems desirable to point out here that the value of c_{nl} depends on details of the shape of the generalized oscillator strength, for all excitation energies, plotted as a function of momentum transfer (Miller and Platzman, 1957; Inokuti, 1971). Also, the wide variation of the derived values of b_K and c_K in Table I is due in large part to relatively small variations in the rate of change of $\sigma_K E_K^2$ as a function of U_K.

We show in Fig. 4 experimental measurements of $\sigma_K E_K^2$ as a function of U_K for a number of low-Z atoms. The measurements of Glupe and Mehlhorn (1967, 1971) for C, N, O, and Ne in Fig. 4(b) show a high degree of internal consistency compared to the several other measurements shown in Fig. 4(a). All measurements of $\sigma_K E_K^2$, however, appear to lie on a common curve (within the estimated accuracy of each experiment) except for the Al measurement of Fischer and Hoffman (1967) and, to a lesser extent, for the measurements for carbon of Hink and Paschke (1971a, 1971b). The experimental data of Glupe and Mehlhorn agree quite well with the theoretical results of McGuire (1971a, 1974) and with the results of Rudge and Schwartz (1966), as shown in Fig. 9.

Fano plots of the experimental measurements for C, N, O, Ne, Al, and Ni are shown in Fig. 5. As pointed out in Sec. IV, the plot for C based on the data of Hink and Paschke (1971a, 1971b) is not linear over the range of U_K found for the other elements, so these data will not be considered further here. Most of the remaining data appear to lie on straight lines for $U_K \gtrsim 4$ ($U_K > 7$ for Ni). For lower values of U_K, the data values lie above the extrapolated straight lines (shown dashed); this trend will be discussed later. The deviation of the Ne points for $U_K > 20$ from the extrapolated line is due to the neglect here of relativistic corrections to the Bethe formula (Inokuti, 1971; Bekk, 1974). The derived Bethe parameters are shown in Table III and it is seen that the overall average value of b_K is about 0.9 while the average value of c_K is about 0.6. This average value of b_K is rather higher than would be expected from the bulk of the theoretical values shown in Table I; the reason for this apparent discrepancy will be discussed in Sec. IX. Some high values of b_K have, however, been obtained from the electron energy-loss experiments referred to in Sec. IV.

We turn now to a comparison of theoretical and experimental cross-section values for ionization of electrons

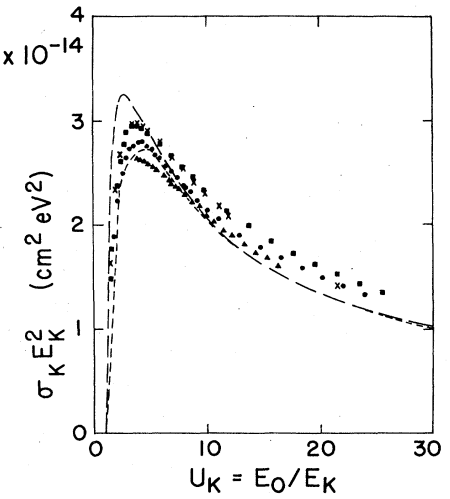

FIG. 9. Comparison of experimental and calculated values of $\sigma_K E_K^2$ as a function of U_K. The experimental points are the data of Glupe and Mehlhorn (1967, 1971), of Glupe (1972), and of Bekk (1974) for C (triangles), Ne (crosses), N (squares), and O (circles), as plotted in Fig. 4(b). The long-dashed line is the result of the calculation by Rudge and Schwartz (1966), while the short-dashed line is the result of the calculation by McGuire (1971a, 1974) for Be, C, and O.

from the L_{23} shell. Figure 2(a) shows a plot of the Worthington–Tomlin equation [Eq. (5)] with $b_L = 0.25$ [as recommended by Mott and Massey (1949)] lying substantially below plots of the Gryzinski (1965) and Drawin (1961) expressions [Eqs. (9) and (10), respectively]; a similar result was found for K-shell ionization (Fig. 8). The result of Lotz (1970), however, is now found to be substantially lower than that found by Gryzinski and Drawin, and the peak in the cross-section curve is much less pronounced. The results of McGuire (1971a, 1974) and Manson (1972, 1974) in Fig. 2(b) are qualitatively similar to the data shown in Fig. 2(a), but the results of McGuire for S and Ar and of Wallace *et al.* (1973) for Ar indicate much higher cross sections than would be expected on the basis of Fig. 2(a).

The experimental data for L_{23}-shell ionization are much more limited than for K-shell ionization. Values of $\sigma_{L_{23}} E_{L_{23}}^2$ are plotted as a function of $U_{L_{23}}$ in Fig. 6. The data of Ogurtsov (1973) for Ar seem to be consistent with the measurements of Vrakking and Meyer (1974) but not with the calculated cross sections of McGuire (1974) and Wallace *et al.* (1973) in Fig. 2(b). Christofzik's (1970) data for Ar, however, are in much closer agreement with the calculations shown for Ar in Fig. 2(b). The results of Vrakking and Meyer (1974) do not agree at all closely, in magnitude and shape, with the calculated curves in Fig. 2(a); better agreement is found with the curves labeled Na and Al (calculated by McGuire) in Fig. 2(b).

Fano plots of the data in Fig. 6 are shown in Fig. 7. As for the case of K-shell ionization (Fig. 5), straight line plots are obtained for $U_{L_{23}} \gtrsim 4$. The derived Bethe parameters are shown in Table IV and are plotted as a function of $E_{L_{23}}$ in Fig. 3. The values of these parameters are generally lower than would be expected from McGuire's (1974) calculations. Experimentally, it would

TABLE IV. Values of Bethe parameters $b_{L_{23}}$ and $c_{L_{23}}$ and their probable errors obtained from the linear least-squares fits to measured L_{23}-shell ionization cross sections for the range of $U_{L_{23}}$ indicated.

Author	Element	Range of $U_{L_{23}}$	$b_{L_{23}}$	$c_{L_{23}}$
Vrakking and Meyer (1974)	P	5.5–18.5	0.38 ± 0.02	0.85 ± 0.10
	S	4.6–15	0.53 ± 0.01	0.55 ± 0.04
	Cl	4.3–12.5	0.65 ± 0.01	0.56 ± 0.02
Ogurtsov (1973)	Ar	4.1–16.3	0.46 ± 0.01	0.63 ± 0.04
Christofzik (1970)	Ar	4–20	0.906 ± 0.003	0.57 ± 0.01

appear that $b_{L_{23}} \approx 0.5$ (Table IV) although it should be kept in mind that the measurements of Vrakking and Meyer were made relative to those of Glupe and Mehlhorn (1967, 1971). The derived values of $c_{L_{23}}$, like those of c_K, are found to be appreciably less than 4. The values of b_{nl} determined from the limited number of electron energy-loss experiments (Sec. IV) appear to be comparable (taking into account the generally rather large errors of measurement) with many of the b_{nl} values shown in Tables I–IV. If, however, values of c_{nl} smaller than 4 were assumed, the b_{nl} values from the energy-loss experiments would tend to be higher than those given in the above four tables.

VIII. DERIVATION OF b_{nl} FROM PHOTOABSORPTION DATA

In view of the paucity of experimental values of σ_{nl} and of the differences noted in the previous section that exist between different results for σ_{nl}, we will now determine values of b_{nl} from experimental photoabsorption data to compare with the values shown in Tables I–IV.

Bethe (1930) has shown that the cross sections for inelastic electron scattering by atoms and ionization by electrons of atoms are related to the cross sections for optical absorption if the incident electron energy is sufficiently large (Fano and Cooper, 1968; Inokuti, 1971). A number of authors (Miller and Platzman, 1957; Durup and Platzman, 1961; Schram *et al.*, 1965; Swanson and Powell, 1968; van der Wiel *et al.*, 1969; Tawara *et al.*, 1973) have made use of this relationship although Tawara *et al.* (1973) have pointed out some apparent discrepancies. The parameter b_{nl} in Eq. (1) can be expressed in the form

$$b_{nl} = \frac{E_{nl}}{Z_{nl}} \int_{E_{nl}}^{\infty} \frac{1}{E} \frac{df}{dE}\, dE\,, \tag{12}$$

where

$$\frac{df}{dE} = \frac{-2E\,\mathrm{Im}(1/\epsilon)}{\pi E_p^2}\,. \tag{13}$$

The quantity df/dE is the differential oscillator strength, at zero momentum transfer, with respect to excitation energy E (Fano, 1956; Glick and Ferrell, 1960), ϵ is the complex dielectric constant (here taken to be a function only of E or of photon energy $\hbar\omega$), and E_p is defined by

$$E_p = \hbar(4\pi N e^2/m)^{1/2} = 28.82(\rho/A)^{1/2}\mathrm{eV}\,. \tag{14}$$

In Eq. (14), N is the number density of atoms (or molecules), ρ is the density (in cgs units), and A is the atomic (or molecular) weight.

The integration in Eq. (12) is performed over that region of differential oscillator strength associated with excitation of electrons from the nl shell, ranging from the threshold energy E_{nl} to some much higher energy, represented here by infinity, where the differential oscillator strength for the nl shell becomes vanishingly small. In practice, the upper limit is sometimes taken as the binding energy of the next most tightly bound shell (or subshell) but it may well happen, particularly for subshells of large values of l, that the differential oscillator strength does not become sufficiently small at this assumed upper limit. The parameter b_{nl} can therefore only be estimated in such cases (Hagemann *et al.*, 1974).

For excitation energies greater than about 50 eV,

$$\epsilon_2 \approx -\mathrm{Im}(1/\epsilon) \tag{15}$$

to better than about 5% (Swanson and Powell, 1968; Hagemann *et al.*, 1974), and to an even better approximation (Hagemann *et al.*, 1974)

$$\int_{E_{nl}}^{\infty} \epsilon_2\, dE \approx -\int_{E_{nl}}^{\infty} \mathrm{Im}\,\frac{1}{\epsilon}\, dE\,, \tag{16}$$

where ϵ_2 is the imaginary part of ϵ. Equation (12) now becomes

$$b_{nl} \approx \frac{2E_{nl}}{\pi Z_{nl} E_p^2} \int_{E_{nl}}^{\infty} \epsilon_2\, dE\,, \tag{17}$$

so that b_{nl} can be estimated from available optical data. The optical constant ϵ_2 can be obtained from x-ray mass absorption coefficients μ_m or photoabsorption cross sections σ_p by use of the relations (Fano and Cooper, 1968)

$$\epsilon_2 = \rho c\hbar\mu_m/E = 1.974\times10^{-5}\rho\mu_m/E\,, \tag{18a}$$

$$\mu_m = N_A\sigma_p/A\,, \tag{18b}$$

and

$$\epsilon_2 = 1.189\times10^{19}\rho\sigma_p/EA\,. \tag{18c}$$

In these equations, N_A is the Avogadro constant, E is expressed in eV, and the other quantities in cgs units.

Theoretical and experimental x-ray absorption data (Hubbell, 1971; Veigele, 1973; Henke and Ebisu, 1974; Hagemann *et al.*, 1974) have been used to estimate b_K and $b_{L_{23}}$ for selected elements using Eqs. (17) and (18). Data in the range of interest from different sources may often differ by up to about 10% so it was considered adequate here to integrate ϵ_2 graphically. The upper limit in Eq. (17) was typically set at about 400 or 500 eV greater than E_{nl} for elements where it was found that ϵ_2

was less than about 1% of the peak value near the threshold. For O, Ne, and Ar it was found necessary to integrate ϵ_2 over a larger range of excitation energy. As an example, Fig. 10 shows a plot of ϵ_2 for Al, based on the data of Hagemann *et al.* (1974), from the threshold for L-shell excitation at 73 eV to 500 eV.

Values of b_K determined for four light elements are shown in Table V. To the estimated accuracy of the x-ray absorption data and the integration, it appears that there is no significant variation with Z and that $b_K = 0.55 \pm 0.05$. This derived value is appreciably lower than the values derived from experimental ionization cross-section data listed in Table III and is also lower than most of the values derived from theoretical cross sections shown in Table I.

Values of $b_{L_{23}}$ for four elements are shown in Table VI. The range of the values is only a little greater than the range of b_K values in Table V but there could be a small systematic variation with Z. These values of $b_{L_{23}}$ are plotted in Fig. 3 and it is seen that the variation with $E_{L_{23}}$ is comparable to that expected from the calculations of McGuire (1974), but less than what could be inferred from the experiments of Vrakking and Meyer (1974) and of Christofzik (1970).

IX. DISCUSSION

We have up to this point implicitly assumed that the Bethe ionization formula [Eqs. (1)–(3)] is valid above some as yet unspecified incident electron energy E_0. The parameters b_{nl} and c_{nl} are considered to be constants for a particular material and electron subshell. We have found empirically that both theoretical and experimental cross-section data can be fitted by the Bethe equation (to an accuracy, sufficient for many purposes, of better than about 1%) for values of U_{nl} greater than about 4 (as exemplified by the Fano plots shown in Figs. 5 and 7).

Examination of soft x-ray absorption data (Hubbell, 1971; Veigele, 1973; Henke and Ebisu, 1974; Hagemann *et al.*, 1974), however, indicates that the differential oscillator strength is not concentrated in a narrow range of excitation energy near a threshold energy E_{nl}. The differential oscillator strength is in fact distributed over an appreciable range of excitation energies extending often up to about $4E_{nl}$ as shown in Fig. 10 for the case of L-shell excitation in Al. It might therefore be expected that Eqs. (1)–(3) would not necessarily be valid until E_0 was much greater than $4E_{nl}$. We must then ask whether the linearity of the Fano plots is fortuitous and whether b_{nl} and c_{nl} should be regarded as functions of U_{nl} for low values of U_{nl}.

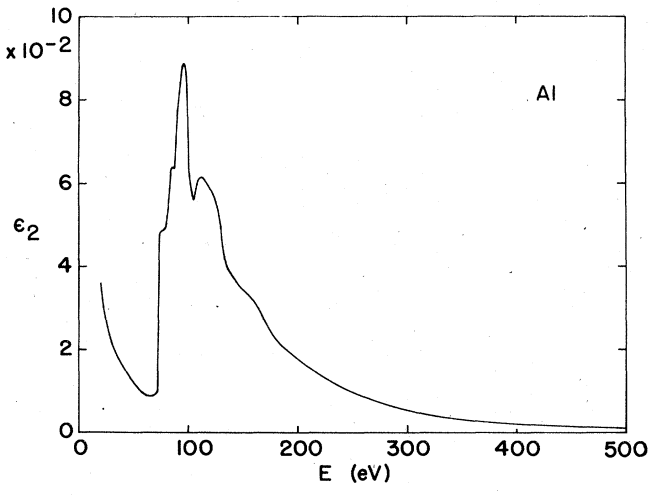

FIG. 10. Plot of the optical constant ϵ_2 for Al as a function of photon (or excitation) energy E (based on the data of Hagemann *et al.*, 1974).

TABLE V. Values of b_K found from x-ray absorption data with use of Eq. (17) and the specified upper limit of integration. The binding energies have been obtained from the compilation of Bearden and Burr (1967).

Element	E_K (eV)	Upper limit (eV)	b_K
Be	111	600	0.58
C	284	700	0.50
O	532	2000	0.55
Ne	867	3000	0.55

We have chosen here to fit ionization cross-section data to Eq. (4) at relatively low values of U_{nl} ($\lesssim 30$) as this is the region of interest in AES and EPMA. Fitting of cross-section data for higher values of U_{nl} could enable us to obtain a "saturated" value of b_{nl} that could be compared validly with a value obtained from photoabsorption data; that is, if U_{nl} was large enough (say 30 to 100), we could be reasonably certain that practically all the available differential oscillator strength was contributing to the observed cross section [cf., Eq. (12)]. The value of c_{nl}, however, would be less precise than we would obtain from fits for lower values of U_{nl}. The derived values of c_{nl} found here, however, are correlated with the values of b_{nl} so a possible energy variation of b_{nl} with U_{nl} at low values of U_{nl} can lead to possibly erroneous values of c_{nl} (that would not be valid at larger values of U_{nl}).

To test the validity of the ideas outlined above, we have arbitrarily put $c_{nl} = 2.42$ (the value expected from the relation $B_{nl} = 1.65E_{nl}$ (Sec. III) recommended by Mott and Massey (1949) and computed an "effective" value of b_{nl} as a function of U_{nl} from the experimental cross-section data. We show in Fig. 11 examples of the trends we have found for all the elements considered here. Figure 11(a) shows a plot of the effective b_K as a function of U_K derived from Glupe and Mehlhorn's (1967, 1971) data for C, N, and O; values of the effective b_K for Ne closely overlap the results for N and, for clarity, have not been shown. Figure 11(b) shows a plot of the effective $b_{L_{23}}$ as

TABLE VI. Values of $b_{L_{23}}$ found from x-ray absorption data with use of Eq. (17) and the specified upper limit of integration.

Element	$E_{L_{23}}$ (eV)	Upper limit (eV)	$b_{L_{23}}$
Al	73	500	0.49
Si	99	600	0.49
S	165	600	0.52
Ar	245	1250	0.61

a function of $U_{L_{23}}$ where we have used Christofzik's (1970) data for Ar and Vrakking and Meyer's (1974) data for P, S, and Cl. These plots show b_{nl} increasing from a low value near threshold and then tending to saturate at a large value of $U_{nl} \gtrsim 20$. This is precisely the trend expected from the previous discussion.

The value we have selected for c_{nl} may not, of course, be "correct" so not much significance should be placed on the numerical values of the effective b_{nl} plotted in Fig. 11. If c_{nl} was put equal to 4, the derived values of b_{nl} would show an increase with increasing U_{nl} similar to that shown in Fig. 11 but would saturate at a lower maximum value; for example, the maximum value of b_K for oxygen would be about 0.54 rather than 0.61. Also, the parameter c_{nl} might be a function of U_{nl} at low values of U_{nl}. Nevertheless, we believe that the general trend of b_{nl} is reasonable considering the known variation of differential oscillator strength. The values of b_K in Fig. 11(a) saturate at a value of about 0.6 (for large U_K), which is close to the value of 0.55 ± 0.05 expected from photoabsorption data (Table V). These values appear to be smaller than the values of b_K ($\approx$0.7 to 0.9 for C, N, and O) derived from electron-scattering experiments (Sec. IV) but, considering the errors of these measurements, the differences may not be significant. Likewise, the curve for Ar in Fig. 11(b) appears to saturate at a value close to the result $b_{L_{23}} = 0.61$ derived from the optical data (Table VI); the extrapolated values of $b_{L_{23}}$ for P, S, and Cl, however, appear to be somewhat lower than the values expected optically.

There is thus a discrepancy between the cross-section measurements of Vrakking and Meyer (1974) and the x-ray absorption data. Although McGuire's (1974) calculations and Vrakking and Meyer's data indicate that $\sigma_{L_{23}}$ varies appreciably with Z (cf., Figs. 2, 3, and 6, and Tables II and IV), this apparent trend is not substantiated by the x-ray absorption data or by the other measurements of $\sigma_{L_{23}}$ referred to in Sec. IV. A more conclusive comparison and analysis would be facilitated by determinations of effective generalized oscillator strengths (in essence, measurements of the effective b_{nl} and c_{nl}) as a function of U_{nl} from electron-scattering experiments.

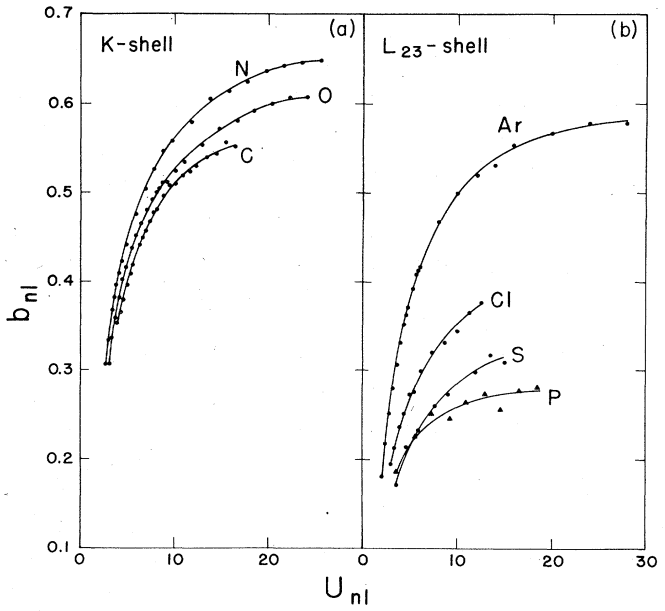

FIG. 11. Plot of the effective value of b_{nl} as a function of U_{nl} found by assuming $c_{nl} = 2.42$. (a) Plot of the effective b_K as a function of U_K using the data of Glupe and Mehlhorn (1971) and of Glupe (1972) for C, N, and O. (b) Plot of the effective $b_{L_{23}}$ as a function of $U_{L_{23}}$ using data of Vrakking and Meyer (1974) for P, S, and Cl and of Christofzik (1970) for Ar. The solid lines have been drawn to show trends indicated by the data values.

It now appears that the values of b_{nl} and c_{nl} derived from experimental cross-section data [from fits to Eq. (4)] and shown in Tables III and IV should only be regarded as empirical parameters describing observed cross sections over a certain range of U_{nl}. These derived values of b_{nl} are systematically higher than those expected optically, for the reasons just discussed. Apparent discrepancies of this type could be more pronounced for subshells with large values of l; for such subshells, the differential oscillator strength may be distributed over a range of excitation energies considerably greater than the threshold E_{nl} (Fano and Cooper, 1968; Henke and Ebisu, 1974). Care should therefore be exercised in interpreting the slope of a Fano plot in a region of low U_{nl} as a measure of the parameter b_{nl} (Tawara *et al.*, 1973). The slope of such a plot would be expected to decrease for larger values of U_{nl} ($\gtrsim$20).

Although the data base in the range of interest here is limited, it is possible to provide "preferred values" of the parameters b_{nl} and c_{nl} for a limited range of U_{nl}. The data of Fig. 4 and the results shown in Table III indicate that there is no appreciable variation in the magnitude of $\sigma_K E_K^2$, for a given U_K, as a function of Z. The empirical parameters listed in Table III ($b_K \approx 0.9$, $c_K \approx 0.65$–0.75) could then be useful for predicting cross sections for other light elements for $4 \lesssim U_K \lesssim 25$. The situation for L_{23}-shell ionization is less certain, for the reasons just discussed. It appears from the bulk of the data referred to in Sec. IV and from x-ray absorption data discussed above that $b_{L_{23}} \approx 0.5$ to 0.6 (for which $c_{L_{23}}$ has usually been assumed to be between 1 and 4). It would be reasonable to expect that future measurements of L-shell ionization cross sections for $4 \lesssim U_L \lesssim 25$ could be described by higher values of b_L and lower values of c_L in the same way that the empirical parameters b_K and c_K suggested above for low U_K differ from those expected from photoabsorption data and the earlier theory (Sec. III). Thus, values of $b_{L_{23}}$ and $c_{L_{23}}$ similar to those derived from Christofzik's (1970) data for Ar (Table IV) might become appropriate for low values of $U_{L_{23}}$. It is clear, however, that better choices of the Bethe parameters can now be made than those recommended many years ago by Mott and Massey (1949).

The discussion up till now has been devoted to the region $U_{nl} \gtrsim 4$ where the Bethe equation is useful. We would now like to examine briefly the region near threshold ($1 \lesssim U_{nl} \lesssim 4$). This region of the cross-section curve needs to be known for quantitative EPMA and AES experiments as inner-shell ionization can be caused not only by incident electrons of energy E_0 but in addition by scattered electrons with energy between E_{nl} and E_0. Not many data exist for this region but it does seem that the

Rudge and Schwartz formula [Eqs. (6) and (7)] describes the near-threshold K-shell cross-section data of Glupe and Mehlhorn (1971) quite well. Care should be used in applying this or other similar formulas as structure in the ionization cross-section curve near threshold has been reported by Gerlach and DuCharme (1974). Also, Smith *et al.* (1974) have found delayed onsets of the cross section for N_{67}-shell ionization in Au, Pb, and Bi analogous to the delayed onsets found in photoabsorption (Fano and Cooper, 1968). The effects on the cross-section curve were very dramatic, with little ionization being observed until $U_{N_{67}}$ reached 1.5–2. We should also note here that the yield of characteristic x rays or Auger electrons from solid samples as a function of E_0 does not simply relate to the ionization cross-section curve on account of scattering (in EPMA) and attenuation of the incident beam and of the effects of backscattered electrons (Neave *et al.*, 1972; Vrakking and Meyer, 1973; Yakowitz, 1974).

Finally, we have assumed throughout this paper that ionization cross-section data for inner-shell electrons for an element in a gas can be applied to the same element in solid form (and vice versa). The general shape of photoabsorption curves as a function of excitation energy in the soft x-ray region does not change appreciably on going from the solid to the gas phase although there can be significant changes in the structure found over small energy ranges (Kunz, 1973). That is, the gross features of photoabsorption appear to be determined by the atomic species and the subshell(s) being excited (Fano and Cooper, 1968). The inner-shell ionization cross section is determined by an energy integration of the optical absorption coefficient [Eqs. (12)–(18)] so that little difference in solid-phase and gas-phase cross sections would be expected.

X. SUMMARY

We have presented a survey of available theoretical and experimental cross-section data for the ionzation of inner-shell electrons of relatively low binding energies (generally less than 1500 eV) by incident electrons of low energy (less than 100 keV but mostly less than 10 keV). Unfortunately, the data base is rather limited so the discussion has been limited to K-shell and L-shell ionization. Nevertheless, it is hoped that the information contained here will be useful for the quantitative analysis of light atoms by electron-probe microanalysis and by Auger-electron spectroscopy. Specific formulas or parameters given here can be used directly or the present and anticipated future data can be used to fix parameters in other analytic models (Green and Stolarski, 1972) for use in transport calculations in correction procedures for quantitative analysis by EPMA and AES.

Calculated, semiempirical, and experimental cross-section data have been intercompared graphically and through fits to the linearized Bethe equation for inner-shell ionization (the Fano plot). Values of the effective Bethe parameters b_{nl} and c_{nl} so derived are listed in Tables I–IV. The data can be satisfactorily fitted over the range $4 \lesssim U_{nl} \lesssim 30$, but it is pointed out that the effective parameters should not be used outside the range of the fit as b_{nl} should more properly be regarded as a function of U_{nl} (for $U_{nl} \lesssim 20$). Values of the parameter b_{nl} have also been derived from photoabsorption data (Tables V and VI) and were found to be consistent with the ionization data if account was taken of distribution of differential oscillator strength and the consequent expected energy variation of b_{nl}. Suggested values for the parameters b_{nl} and c_{nl} for K-shell and L_{23}-shell ionization in the range $4 \lesssim U_{nl} \lesssim 25$ are given in Sec. IX.

Experimental values of $\sigma_K E_K^2$ appeared to lie on a common curve when plotted as a function of U_K. These values agree quite well with the theoretical results of Rudge and Schwartz (1966) for $5 < U_K < 26$ and the results of McGuire (1971a, 1974). It therefore appears that cross sections for other light atoms can be obtained by appropriate scaling.

A greater spread exists in the plots of calculated and measured values of $\sigma_{L_{23}} E_{L_{23}}^2$ as a function of $U_{L_{23}}$ than for the case of K-shell ionization. A significant variation in the magnitude of $\sigma_{L_{23}} E_{L_{23}}^2$ as a function for Z (for a given value of $U_{L_{23}}$) is apparent in the experimental data of Vrakking and Meyer (1974) and in the calculations of McGuire (1974). This variation leads to a large variation in the magnitude of the Bethe parameter $b_{L_{23}}$ as a function of Z that is not substantiated by either the results of many photoabsorption experiments or by the limited number of L-shell ionization cross sections derived from characteristic x-ray and Auger-electron yield experiments. More cross-section measurements are required to resolve this discrepancy and to better define the variation of $\sigma_{L_{23}} E_{L_{23}}^2$ with Z.

The relatively simple and widely used expressions of Gryzinski (1965), Drawin (1961, 1963), and Lotz (1970) agree closely with each other (within 10%) in the case of K-shell ionization for $U_K < 30$ (Fig. 8). These results, however, appear to lie roughly 10%–15% lower than the experimental data shown in Fig. 4. For the case of L_{23}-shell ionization, the Lotz expression is substantially different from the Gryzinski and Drawin results (which agree well with each other). The latter results agree closely with the cross-section measurements of Christofzik (1970) for Ar.

There are few measurements (e.g., Vrakking and Meyer, 1974) of cross sections for ionization from the M, N, and O shells of medium- and high-Z atoms. It is hoped that this deficiency can be corrected in the near future.

Note added in proof: The calculations of Arthurs and Moiseiwitsch (1958) have been extended to higher energies and to heavier atoms by Davidović and Moiseiwitsch (1975). The new values of σ_K for low- and medium-Z atoms, of interest here, are greater than the previous results shown in Fig. 1(b) by ≈30% for Ni, and by ≈60% for Al.

Cosslett and Leapman (1975) have obtained inner-shell ionization cross sections from measurements of the energy-loss spectra of 60 keV electrons transmitted through thin films of C, Al, Cr, Fe, Cu, and Ag. These measurements yielded the following values of b_{nl} (with estimated uncertainties of ±15-30%) if c_{nl} was assumed to be 4 (Sec. IV): $b_K = 0.48$ for C and Al; $b_{L_{23}} = 0.44$, 0.37, and 0.34 for Cr, Fe, and Cu, respectively; and $b_{M_{45}} = 0.10$ for Ag. The derived values of b_K are in moderate agreement with those obtained from photoabsorption experiments (Table V) but the derived values of

$b_{L_{23}}$ are lower than those shown in Table VI. The measured L_{23}-shell ionization cross sections do not substantiate the Z variation of the cross sections that was reported by Vrakking and Meyer (1974) and discussed in Sec. IX.

Quarles (1975) has analyzed values of σ_K measured over a wide range of U_K and Z with the use of the Bethe equation [Eq. (1)]. This analysis shows that $b_K = 0.64$ (c_K was assumed to be 1) with no detectable variation of b_K with Z, a result consistent with the bulk of the data discussed in Secs. IV, VIII, and IX.

ACKNOWLEDGMENTS

The author is particularly indebted to Dr. R. L. Gerlach, Dr. C. Kunz, Dr. S. T. Manson, Dr. E. J. McGuire, Dr. W. Mehlhorn, and Dr. C. A. Quarles who have graciously communicated data in advance of publication. He also wishes to thank them and J. W. Cooper for helpful discussions or correspondence.

REFERENCES

Andersen, C. A., 1972, Editor, *Microprobe Analysis* (Wiley, New York).
Arthurs, A. M., and B. L. Moiseiwitsch, 1958, Proc. R. Soc. London A **247**, 550.
Azâroff, L. V., and D. M. Pease, 1974, in *X-ray Spectroscopy*, edited by L. V. Azâroff (McGraw-Hill, New York), p. 284.
Bambynek, W., B. Crasemann, R. W. Fink, H.-U. Freund, H. Mark, C. D. Swift, R. E. Price, and P. V. Rao, 1972, Rev. Mod. Phys. **44**, 716.
Bearden, J. A., and A. F. Burr, 1967, Rev. Mod. Phys. **39**, 78.
Bekk, K.-J., 1974, Diplom-Thesis, University of Freiburg.
Bell, K. L., and A. E. Kingston, 1974, in *Advances in Atomic and Molecular Physics*, edited by D. R. Bates and B. Bederson (Academic, New York), Vol. 10, p. 53.
Bethe, H., 1930, Ann. Phys. **5**, 325.
Birks, L. S., 1971, *Electron Probe Microanalysis* (Wiley-Interscience, New York), second edition.
Brown, D. B., and J. V. Gilfrich, 1971, J. Appl. Phys. **42**, 4044.
Burgess, A., and I. Percival, 1968, in *Advances in Atomic and Molecular Physics*, edited by D. R. Bates and I. Estermann (Academic, New York), Vol. 4, p. 109.
Burhop, E. H. S., 1940, Proc. Camb. Philos. Soc. **36**, 43.
Carlson, T. A., W. E. Hunt, and M. O. Krause, 1966, Phys. Rev. **151**, 41.
Carlson, T. A., W. E. Moddeman, and M. O. Krause, 1970, Phys. Rev. A **1**, 1406.
Chang, C. C., 1974, in *Characterization of Solid Surfaces*, edited by P. F. Kane and G. B. Larrabee (Plenum, New York), p. 509.
Chang, C. C., 1975, Surf. Sci. **48**, 9.
Christofzik, H.-J., 1970, Diplom-Thesis, University of Münster.
Clark, J. C., 1935, Phys. Rev. **48**, 30.
Codling, K., 1973, Rep. Prog. Phys. **36**, 541.
Colliex, C., and B. Jouffrey, 1972, Phil. Mag. **25**, 491.
Cooper, J. W., 1973, in *Proceedings of the International Conference on Inner Shell Ionization Phenomena and Future Applications*, edited by R. W. Fink, S. T. Manson, J. M. Palms, and P. V. Rao (U. S. Atomic Energy Commission, Oak Ridge, Tenn., CONF-720404), Vol. 2, p. 807.
Cosslett, V. E., and R. D. Leapman, 1975, private communication.
Dangerfield, G. R., and B. M. Spicer, 1975, J. Phys. B **8**, 1744.
Davidović, D. M., and B. L. Moiseiwitsch, 1975, J. Phys. B **8**, 947.
Davis, D. V., V. D. Mistry, and C. A. Quarles, 1972, Phys. Lett. **38A**, 169.
Dehmer, J. L., and R. P. Saxon, 1973, Argonne National Laboratory Rep. No. ANL-8060, p. 102.
Drawin, H.-W., 1961, Z. Phys. **164**, 513.
Drawin, H.-W., 1963, Z. Phys. **172**, 429.
DuCharme, A. R., and R. L. Gerlach, 1973, J. Vac. Sci. Technol. **10**, 188.
Durup, J., and R. L. Platzman, 1961, Discuss. Faraday Soc. **31**, 156.
Egerton, R. F., 1975, Phil. Mag. **31**, 199.
Ehrhardt, H., K. H. Hesselbacher, K. Jung, and K. Willman, 1972, in *Case Studies in Atomic Collision Physics II*, edited by E. W. McDaniel and M. R. C. McDowell (North-Holland, Amsterdam), p. 161.
Fano, U., 1954, Phys. Rev. **95**, 1198.
Fano, U., 1956, Phys. Rev. **103**, 1202.
Fano, U., and J. W. Cooper, 1968, Rev. Mod. Phys. **40**, 441.
Fischer, B., and K.-W. Hoffmann, 1967, Z. Phys. **204**, 122.
Fong, L. H., and S. G. Tomlin, 1970, Aust. J. Phys. **23**, 17.
Gallon, T. E., 1972, J. Phys. D. **5**, 822.
Gerlach, R. L., and A. R. DuCharme, 1972, Surf. Sci. **32**, 329.
Gerlach, R. L., and A. R. DuCharme, 1974, Jpn. J. Appl. Phys. Suppl. **2**, Pt. 2, 675.
Glick, A. J., and R. A. Ferrell, 1960, Ann. Phys. (N.Y.) **11**, 359.
Glupe, G., 1972, Ph.D. Thesis, University of Münster.
Glupe, G., and W. Mehlhorn, 1967, Phys. Lett. **25A**, 274.
Glupe, G., and W. Mehlhorn, 1971, J. Phys. (Paris) **C4**, 40.
Goldstein, J. I., 1974, in *Practical Scanning Electron Microscopy, Electron and Ion Microprobe Analysis*, edited by J. I. Goldstein and H. Yakowitz (Plenum, New York), p. 49.
Green, A. E. S., and R. S. Stolarski, 1972, J. Atmos. Terr. Phys. **34**, 1703.
Green, M., and V. E. Cosslett, 1961, Proc. Phys. Soc. London **78**, 1206.
Green, M., and V. E. Cosslett, 1968, J. Phys. D **1**, 425.
Gryzinski, M., 1965, Phys. Rev. Sect. A **138**, 336.
Hagemann, H.-J., W. Gudat, and C. Kunz, 1974, Deutsches Elektronen-Synchrotron Report DESY SR-74/7.
Hansen, H., H. Weigmann, and A. Flammersfeld, 1964, Nucl. Phys. **58**, 241.
Hansen, H., and A. Flammersfeld, 1966, Nucl. Phys. **79**, 135.
Henke, B. L., and E. S. Ebisu, 1974, in *Advances in X-ray Analysis*, edited by C. L. Grant, C. S. Barrett, J. B. Newkirk, and C. O. Ruud (Plenum, New York), Vol. 17, p. 150.
Hink, W., 1964, Z. Phys. **177**, 424.
Hink, W., 1965, Z. Phys. **182**, 227.
Hink, W., J. Jessenberger, and A. Ziegler, 1969, Z. Phys. **226**, 463.
Hink, W., and H. Paschke, 1971a, Z. Phys. **244**, 140.
Hink, W., and H. Paschke, 1971b, Phys. Rev. A **4**, 507.
Hink, W., and A. Ziegler, 1969, Z. Phys. **226**, 222.
Hubbell, J. H., 1971, At. Data **3**, 241.
Hutchins, G. A., 1974, in *Characterization of Solid Surfaces*, edited by P. F. Kane and G. B. Larrabee (Plenum, New York), p. 441.
Inokuti, M., 1971, Rev. Mod. Phys. **43**, 297.
Inokuti, M., R. P. Saxon and J. L. Dehmer, 1975, Int. J. Radiat. Phys. Chem. **7**, 109.
Isaacson, M., 1972, J. Chem. Phys. **56**, 1813.
Isaacson, M., and D. Johnson, 1975, Ultramicroscopy **1**, 33.
Kieffer, L. J., 1969, At. Data **1**, 19.
Kieffer, L. J., and G. H. Dunn, 1966, Rev. Mod. Phys. **38**, 1.
Kolbenstvedt, H., 1967, J. Appl. Phys. **38**, 4785.
Kunz, C., 1973, Comments Solid State Phys. **5**, 31.
Lifshin, E., 1974, in *Scanning Electron Microscopy* by O. C. Wells, A. Boyde, E. Lifshin, and A. Rezanowich (McGraw-Hill, New York), p. 243.
Lotz, W., 1967, Z. Phys. **206**, 205.

Lotz, W., 1968, Z. Phys. **216**, 241.
Lotz, W., 1969, Z. Phys. **220**, 466.
Lotz, W., 1970, Z. Phys. **232**, 101.
Madison, D. H., and E. Merzbacher, 1975, in *Atomic Inner-Shell Processes*, edited by B. Crasemann, Vol. 1, *Ionization and Transition Probabilities* (Academic, New York), p. 1.
Manson, S. T., 1972, Phys. Rev. A **6**, 1013.
Manson, S. T., 1974, private communication.
Massey, H. S. W., and E. H. S. Burhop, 1969, *Electronic and Ionic Impact Phenomena* (Oxford University, London), Vol. 1, Chap. 3.
McGuire, E. J., 1971a, J. Phys. (Paris) **C4**, 37.
McGuire, E. J., 1971b, Phys. Rev. A **3**, 267.
McGuire, E. J., 1974, private communication.
Meyer, F., and J. J. Vrakking, 1973, Phys. Lett. **44A**, 511.
Miller, W. F., and R. L. Platzman, 1957, Proc. Phys. Soc. London A **70**, 299.
Mohr, C. B. O., 1968, in *Advances in Atomic and Molecular Physics*, edited by D. R. Bates and I. Estermann (Academic, New York), Vol. 4, p. 221.
Morabito, J. M., 1975, Surf. Sci. **49**, 318.
Mott, N. F., and H. S. W. Massey, 1949, *The Theory of Atomic Collisions* (Oxford University, London), second edition, pp. 243–244.
Motz, J. W., and R. C. Placious, 1964, Phys. Rev. Sect. A **136**, 662.
Neave, J. H., C. T. Foxon, and B. A. Joyce, 1972, Surf. Sci. **29**, 411.
Ogurtsov, G. N., 1973, Sov. Phys.–JETP **37**, 584 [Zh. Eksp. Teor. Fiz. **64**, 1149 (1973)].
Palmberg, P. W., 1973, Anal. Chem. **45**, 549A.
Perlman, H. S., 1960, Proc. Phys. Soc. London **76**, 623.
Pessa, V. M., and W. R. Newell, 1971, Phys. Scr. **3**, 165.
Peterkop, R., and V. Veldre, 1966, in *Advances in Atomic and Molecular Physics*, edited by D. R. Bates and I. Estermann (Academic, New York), Vol. 2, p. 263.
Pockman, L. T., D. L. Webster, P. Kirkpatrick, and H. Harworth, 1947, Phys. Rev. **71**, 330.
Powell, C. J., 1974, Surf. Sci. **44**, 29.
Powell, C. J., R. J. Stein, P. B. Needham, Jr., and T. J. Driscoll, 1975, Bull. Am. Phys. Soc. **20**, 863.
Quarles, C. A., 1975, in *Electronic and Atomic Collisions*, Ninth International Conference on the Physics of Electronic and Atomic Collisions, Seattle, 1975, edited by J. S. Risley and R. Geballe (University of Washington Press, Seattle), p. 898.
Reed, S. J. B., 1975, *Electron Microprobe Analysis* (Cambridge University, London).
Rester, D. H., and W. E. Dance, 1966, Phys. Rev. **152**, 1.
Riviere, J. C., 1973, Contemp. Phys. **14**, 513.
Reuter, W., 1971, Surf. Sci. **25**, 80.
Rudge, M. R. H., 1968, Rev. Mod. Phys. **40**, 564.
Rudge, M. R. H., and S. B. Schwartz, 1966, Proc. Phys. Soc. London **88**, 563.
Schram, B. L., F. J. de Heer, M. J. van der Wiel, and J. Kistemaker, 1965, Physica **31**, 94.
Schram, B. L., and L. Vriens, 1965, Physica **31**, 1431.
Seah, M. P., 1973, Surf. Sci. **40**, 595.
Severly, J., J. Ph. Perez, Y. Kihn, and B. Jouffrey, 1974, in *Vacuum Ultraviolet Radiation Physics*, edited by E.-E. Koch, R. Haensel, and C. Kunz (Pergamon, New York, and Vieweg, Braunschweig), p. 618.
Smick, A. E., and P. Kirkpatrick, 1945, Phys. Rev. **67**, 153.
Smith, D. M., and T. E. Gallon, 1974, J. Phys. D **7**, 151 (1974).
Smith, D. M., T. E. Gallon, and J. A. D. Matthew, 1974, J. Phys. B **7**, 1255.
Staib, P., and J. Kirschner, 1974, Appl. Phys. **3**, 421.
Swanson, N., and C. J. Powell, 1968, Phys. Rev. **167**, 592.
Tawara, H., K. G. Harrison, and F. J. de Heer, 1973, Physica **63**, 351.
van der Wiel, M. J., 1973, in *The Physics of Electronic and Atomic Collisions*, Eighth International Conference on the Physics of Electronic and Atomic Collisions, Beograd, 1973, edited by B. C. Cobic and M. V. Kurepa (Institute of Physics, Beograd, Yugoslavia), p. 417.
van der Wiel, M. J., T. M. El-Sherbini, and L. Vriens, 1969, Physica **42**, 411.
Veigele, W. J., 1973, At. Data **5**, 51.
Vrakking, J. J., and F. Meyer, 1973, Surf. Sci. **35**, 34.
Vrakking, J. J. and F. Meyer, 1974, Phys. Rev. A **9**, 1932.
Vrakking, J. J., and F. Meyer, 1975, Surf. Sci. **47**, 50.
Vriens, L., 1969, in *Case Studies in Atomic Collision Physics I*, edited by E. W. McDaniel and M. R. C. McDowell (North-Holland, Amsterdam), p. 335.
Wallace, S. J., R. A. Berg, and A. E. S. Green, 1973, Phys. Rev. A **7**, 1616.
Webster, D. L., W. W. Hansen, and F. B. Duveneck, 1933, Phys. Rev. **43**, 851.
Worthington, C. R., and S. G. Tomlin, 1956, Proc. Phys. Soc. London A **69**, 401.
Yakowitz, H., 1974, in *Practical Scanning Electron Microscopy, Electron and Ion Microprobe Analysis*, edited by J. I. Goldstein and H. Yakowitz (Plenum, New York), p. 327 and p. 373.